THE FASEB JOURNAL • RESEARCH • www.fasebj.org

Cigarette smoke modifies and inactivates SPLUNC1, leading to airway dehydration

Patrick J. Moore,* Boris Reidel,* Arunava Ghosh,* Juliana Sesma,† Mehmet Kesimer,* and Robert Tarran*,‡,1
*Marsico Lung Institute and ‡Department of Cell Biology and Physiology, University of North Carolina at Chapel Hill, North Carolina, USA; and †Spyryx Biosciences, Durham, North Carolina, USA

ABSTRACT: Chronic obstructive pulmonary disease (COPD) is a growing cause of morbidity and mortality worldwide. Cigarette smoke (CS) exposure, a major cause of COPD, dysregulates airway epithelial ion transport and diminishes airway surface liquid (ASL) volume. Short palate lung and nasal epithelial clone 1 (SPLUNC1) is secreted into the airway lumen where it maintains airway hydration via interactions with the epithelial Na^+ channel (ENaC). Although ASL hydration is dysregulated in CS-exposed/COPD airways, effects of CS on SPLUNC1 have not been elucidated. We hypothesized that CS alters SPLUNC1 activity, therefore contributing to ASL dehydration. CS exposure caused irreversible SPLUNC1 aggregation and prevented SPLUNC1 from internalizing ENaC and maintaining ASL hydration. Proteomic analysis revealed αβ-unsaturated aldehyde modifications to SPLUNC1's cysteine residues. Removal of these cysteines prevented SPLUNC1 from regulating ENaC/ASL volume. In contrast, SPX-101, a peptide mimetic of natural SPLUNC1, that internalizes ENaC, but does not contain cysteines was unaffected by CS. SPX-101 increased ASL hydration and attenuated ENaC activity in airway cultures after CS exposure and prolonged survival in a chronic airway disease model. These findings suggest that the CS-induced defects in SPLUNC1 can be circumvented, thus making SPX-101 a novel candidate for the treatment of mucus dehydration in COPD. —Moore, P. J., Reidel, B., Ghosh, A., Sesma, J., Kesimer, M., Tarran, R. Cigarette smoke modifies and inactivates SPLUNC1, leading to airway dehydration. FASEB J. 32, 000–000 (2018). www.fasebj.org

KEY WORDS: BPIFA1 · αβ-unsaturated aldehydes · airway surface liquid · ENaC · COPD

Cigarette smoke (CS) contains a complex mixture of more than 5000 chemicals that can interact with airway epithelia (1). Harmful, volatile constituents of tobacco smoke include acetaldehyde, acrolein, and crotonaldehyde (2). Of note, crotonaldehyde and acrolein are 2 of the strongest electrophiles among αβ-unsaturated aldehydes that are present in CS and CS extract and can cause DNA and protein adduct formation (3, 4). Indeed, inhalation of CS introduces exogenous reactive oxidants into the airways and causes the generation of endogenous oxidants that are released by the lung (5). For example, acrolein from CS can induce adduct formation on surfactant protein A, which results in a loss of function and decreased levels of surfactant protein A in patients with chronic obstructive pulmonary disease (COPD) compared with healthy individuals (6, 7). Furthermore, acrolein modifies extracellular matrix proteins and reduces their ability to interact with macrophages, which results in decreased phagocytosis of apoptotic neutrophils (8). Acrolein also forms adducts with apolipoprotein E, which results in changes in protein folding and a loss of function (9).

COPD is the fourth leading cause of death worldwide and is most often caused by chronic CS exposure (10). COPD manifests as 2 major phenotypes, emphysema and chronic bronchitis (CB). The CB form of COPD is characterized by chronic airway inflammation and an increase in mucus production that results in irreversible airflow obstruction and a subsequent decline in lung function (11, 12). Although current therapies, such as anti-inflammatory and bronchodilator therapies, are available, they fail to stop disease progression, and, at present, there is no cure for CB/COPD. Located at the interface between the host and the environment, the airway surface liquid (ASL) represents the first line of defense against inhaled CS toxicants. ASL volume homeostasis is controlled by cystic fibrosis transmembrane conductance regulator (CFTR) –mediated anion secretion and epithelial Na^+ channel (ENaC) –mediated Na^+ absorption (13). CS exposure has been shown to inhibit CFTR without inhibiting ENaC, which leads to ASL dehydration (14–17). ASL/mucus dehydration leads to a failure to clear mucus from the lung and an increase in mucus plugging. Indeed, ASL

ABBREVIATIONS: ASL, airway surface liquid; CB, chronic bronchitis; CF, cystic fibrosis; CFTR, cystic fibrosis transmembrane conductance regulator; COPD, chronic obstructive pulmonary disease; CS, cigarette smoke; ENaC, epithelial Na^+ channel; FBS, fetal bovine serum; GFP, green fluorescent protein; HA, hemagglutinin; HBEC, human bronchial epithelial cell; SPLUNC1, short-palate, lung and nasal epithelial clone 1

[1] Correspondence: Marsico Lung Institute, University of North Carolina at Chapel Hill, 7102 Marsico Hall, 125 Mason Farm Rd., Chapel Hill, NC 27599, USA. E-mail: robert_tarran@med.unc.edu

doi: 10.1096/fj.201800345R

dehydration closely correlates with the decline in FEV_1 in patients with COPD, which suggests that restoring ASL hydration may be beneficial for these patients (18).

The short palate, lung, and nasal epithelial clone 1 (SPLUNC1), also known as bactericidal/permeability increasing family member A1 (BPIFA1), is a 256-aa protein secreted into the airway lumen (19). SPLUNC1 negatively regulates ENaC to limit ASL absorption (20). This interaction occurs *via* the N-terminal S18 region of SPLUNC1 and the β-subunit of ENaC (21); however, additional domains on the main body of SPLUNC1 can also influence this interaction. For example, we have previously demonstrated that pH-sensitive salt bridges on SPLUNC1 modulate the ability of the S18 region to bind to ENaC (22). SPLUNC1 also contains 2 cysteine residues at positions 180 and 224 that may form intermolecular disulfide bonds (21). Although salt bridges play a critical role in ENaC regulation, the role of disulfide bonds in the ability of SPLUNC1 to modulate ENaC and ASL volume is less clear.

SPX-101 is a novel peptide mimetic of natural SPLUNC1 that induces ENaC internalization to attenuate transepithelial Na^+ absorption, thereby increasing ASL hydration (23). SPX-101 increased survival rates in β-ENaC–overexpressing transgenic mice that spontaneously developed lung disease (23, 24) and restored mucus transport in an ovine model in which CFTR was pharmacologically inhibited (23). As patients with COPD suffer from mucus dehydration as a result of mucus hypersecretion and reduced levels of CFTR, SPX-101 may serve as a novel therapy with which to treat individuals with CB/COPD. Although the biologic effects of CS are diverse, few studies have examined the effects of CS on secreted airway proteins. Here, we tested the hypothesis that CS exposure adversely affects the structure/function of SPLUNC1, which contributes to CS-induced ASL dehydration, and that this dysregulation can be restored with the addition of SPX-101.

MATERIALS AND METHODS

SPLUNC1 purification

A plasmid that contained SPLUNC1 cDNA was transformed into BL21-CodonPlus competent cells (Agilent Technologies, Santa Clara, CA, USA) and purified as previously described (21). After purification, all recombinant SPLUNC1 proteins were produced as described previously and stored at −80°C until required (21). Recombinant SPLUNC1 proteins tested here included $SPLUNC1^{\Delta 19}$, which lacks the cleavable N-terminal signal sequence (residues M1–M19) but is otherwise full length (referred to as rSPLUNC1). $rSPLUNC1^{C180A}$, $rSPLUNC1^{C224A}$, and $rSPLUNC1^{C180A/C224A}$ were generated using $rSPLUNC1^{\Delta 19}$ by site-derived mutagenesis and where noted were labeled with the Dylight NHS Ester Dyes (Thermo Fisher Scientific, Waltham, MA, USA) according to the manufacturer's protocol.

CS exposure

Human bronchial epithelial cultures (HBECs) were placed in a chamber that exposed apical surfaces, but not basolateral surfaces, to CS (25). CS was then generated from Kentucky Research cigarette (3R4F) by generating a 35-ml draw over 2 s using a smoke engine (Borgwaldt, Richmond, VA, USA) applied to cultures at a rate of 1 puff every 30 s until the cigarette was exhausted (~13 puffs over ~5 min). This protocol has previously been shown to internalize CFTR from the plasma membrane without inducing cellular toxicity (16). To investigate the effect of rSPLUNC1 under cell-free conditions, protein was dissolved in Ringer's solution and 100 μl of this solution was placed in a petri dish and exposed to 13 puffs over 5 min. To determine whether the effects of CS were reversible, Ringer's solution, CS Ringer's solution, rSPLUNC1 (40 μM), and CS rSPLUNC1 (40 μM) were dialyzed overnight in 10-kDa dialysis cassette (Thermo Fisher Scientific) in buffer (11.57 mM $Na_2HPO_4 0.7H_2O$, 79 mM NaH_2PO_4, 150 mM NaCl). For SPX-101 ASL experiments, SPX-101 (10 μM) was exposed to CS under cell-free conditions in the smoke chamber and subsequently added apically to HBECs. To examine the prophylactic effects of SPX-101 on CS, exposed HBECs were pretreated with SPX-101 for 30 min and HBECs were exposed to CS (17). For ASL height recovery studies, cells were treated with CS for ~5 min and placed in an incubator for 30 min before addition of SPX-101 as a suspension in perfluorocarbon (MilliporeSigma, Burlington, MA, USA) as previously described (26).

HBEC mucosal binding assay

For the HBEC mucosal binding assay, rSPLUNC1 protein was labeled with amine-reactive Dylight 633 (Thermo Fisher Scientific) per the manufacturer's instructions. Dexamethasone (100 nM; MilliporeSigma) was added basolaterally to HBECs 24 h before the experiment. On the day of the experiment, HBECs were washed mucosally with PBS and fresh media was added serosally. Cells were loaded with calcein-AM (Thermo Fisher Scientific) for 30 min before apical addition of fluorescently labeled SPLUNC1. Fluorescent SPLUNC1 and CS SPLUNC1 (40 μM) was added apically in 20 μl modified Ringer's solution and incubated for 6 h at 37°C. Cultures were then washed mucosally 3 times with 500 μl of 4°C PBS to remove unbound rSPLUNC1, and serosal media was replaced with 4°C medium. Cultures were then imaged using a Leica SP8 confocal microscope Leica Microsystems, Wetzlar, Germany) with a ×63 glycerol immersion objective. Dylight 633 fluorescence was acquired using a He-Ne 633 nm laser, with emission collected from 640–680 nm.

ASL height measurements

ASL height was measured on HBECs that had been grown under air-liquid interface conditions for 3–4 wk and subsequently washed twice with 500 μl of PBS for 30 mins to remove endogenous ASL as described (27). HBECs were incubated with 20 μl Ringer's solution that contained 40 μM rSPLUNC1 or Ringer's solution (control) as indicated. In all cases, 10 kDa tetramethylrhodamine dextran (Thermo Fisher Scientific) at 1 mg/ml was added to label the ASL. After 6 h at 37°C, ASL height was measured using 10 predetermined points on a Leica SP5 confocal microscope with a ×63 glycerol immersion objective as previously described (21). Perfluorocarbon was added apically before imaging to prevent ASL evaporation (13).

Western blot assays

Purified rSPLUNC1 was exposed to air or CS and denatured using 2-ME (MilliporeSigma). Samples were separated by SDS-PAGE and transferred to PVDF membranes. Membranes were blocked with 5% skimmed milk in Tris-buffered saline with Tween 20 for 1 h at room temperature and were then incubated with a SPLUNC1 Ab (R&D Systems, Minneapolis, MN, USA) diluted 1:5000 with 5% milk at 4°C overnight. Horseradish

peroxidase–conjugated anti-goat Ab was used as secondary Ab to detect rSPLUNC1 by ECL (Thermo Fisher Scientific). Where indicated, samples were loaded onto nonreducing PAGE gels according to the manufacturer's instructions (Thermo Fisher Scientific).

Cell culture and transfection

Normal human or COPD donor lungs and excised recipient lungs of normal patients were obtained at the time of lung transplantation from main stem/lobar bronchi by enzymatic digestions using protocols approved by the University of North Carolina Committee on the Protection of the Rights of Human Subjects. HBECs were grown from cells that were harvested by enzymatic digestion of human bronchial tissue and cultured on 12-mm Transwell permeable supports (Corning, New York, NY, USA) and maintained at an air-liquid interface for ~4 wk in UNC air-liquid interface media at 37°C/5% CO_2 as described in Randell *et al.* (28). All experiments were performed within 4 wk after seeding.

HEK293T cells were cultured in DMEM medium with 10% fetal bovine serum (FBS), 1× penicillin/streptomycin at 37° with 5% CO_2. For surface biotinylation experiments, HEK293T cells were seeded on Corning tissue culture–treated 60 × 15 mm-dishes. HEK293T cells were transfected using Lipofectamine 2000 (Thermo Fisher Scientific) according to the manufacturer's instructions when cells were 70% confluent 12 h before the experiment. For each construct, 1 μg/DNA was used to transfect 60 × 15 mm dishes, and 3 μg/DNA were used to transfect 10-cm plates. Human wild-type α-, β-, and γ-ENaC constructs were used in combinations of tagged and untagged subunits. For double-tagged subunits, human α-, β-, and γ-ENaC were each tagged with hemagglutinin (HA) on the N terminus and with V5 on the C terminus as previously described (29, 30). For fluorescent reading, α-ENaC and CFTR were tagged with green fluorescent protein (GFP) on their C termini, which were gifts from Dr. Deborah Baines (St. George's University, London, United Kingdom) (31). The GFP-CFTR construct was donated by Dr. Bruce Stanton (Dartmouth College, Hanover, NH, USA) (31).

Surface biotinylation

HEK293T cells were transfected with: *1*) human HA-αENaC-V5, β-, and γ-ENaC; *2*) human αENaC, HA-βENaC-V5, and γENaC; and *3*) human α-, β-ENaC, and HA-γENaC-V5 (4). Cells were treated with 40 μM SPLUNC1 in DMEM with 10% FBS at 37°C/5% CO_2 for 1 h. Cells were washed with ice-cold PBS with 1 mM $MgCl_2$ and 1 mM CaCl (PBS^{2+}). Cells were incubated with 0.5 mg/ml NHS-Biotin (Thermo Fisher Scientific) in borate buffer for 20 min under gentle agitation on ice. Biotinylation was quenched with 10% FBS in PBS^{2+} for 20 min on ice under gentle agitation. Cells were lysed with 100–200 μl biotinylation lysis buffer [10 mM TRIS-HCl (pH 7.4), 0.4% sodium deoychorate, 1% NP-40, and 50 mM EGTA with protease inhibitor cocktail; Roche, Basel, Switzerland]. Lysed cells were incubated on ice for 30 min and centrifuged for 10 min at 5000 *g*. Supernatants were subjected to bicinchoninic acid protein assay (Thermo Fisher Scientific), and an equal amount of protein was incubated with 125 μl of Neutravidin agarose (Thermo Fisher Scientific) under invert rotation. Neutravidin beads were washed 3 times with PBS^{2+}, and proteins were eluted using 2× Laemmli sample buffer (Bio-Rad, Hercules, CA, USA) by boiling at 95°C for 10 min. After cooling down, Neutravidin beads were separated from eluted proteins by centrifugation at 14,000 *g* for 3 min at room temperature. Supernatants were subjected to SDS-PAGE. Anti-V5 (Thermo Fisher Scientific) and anti–glyceraldehyde 3-phosphate dehydrogenase (Santa Cruz Biotechnology, Dallas, TX, USA) Abs were used for immunoblotting.

Microelectrode studies

A single-barreled transepithelial potential difference (V_t) –sensing microelectrode was positioned in the ASL by micromanipulator and used in conjunction with a macroelectrode in the serosal solution to measure V_t with a voltmeter (World Precision Instruments, Sarasota, FL, USA) as previously described (26). All experiments were performed with 10 μM bumetanide (MilliporeSigma) added serosally to inhibit chloride secretion. Perfluorocarbon was added to the mucosal surface during the period of recording to avoid ASL evaporation.

Internalization assay

HEK293T cells were cultured in 10-cm dishes and subsequently transfected overnight with αENaC-GFP, β-, and γ-ENaC, and CFTR-GFP. Cells were trypsinized and seeded in a 96-well plate at a density of 60,000 cells/well and incubated for 8 h at 37°C and 5% CO_2 to allow cells to recuperate. On the same day, cells were incubated with Ringer's solution, CS Ringer's solution, 40 μM rSPLUNC1, and CS rSPLUNC1 for 1 h at 37°C/5%CO_2. Ten micromolar SPX-101 and CS-SPX-101, and 1 μM crotonaldehyde (MilliporeSigma) was also added for 1 h at 37°C/5% CO_2. Fluorescence was read using a Tecan Infinite M1000 Multiplate Reader (Tecan Group, Männedorf, Switzerland) at 37°C.

Mass spectrometry analysis

CS- and air control–exposed rSPLUNC1 (40 μM) and SPX-101 (10 μM) were immediately prepared for mass spectrometry analysis by filter-aided sample preparation (33). First, each sample was spin filtered at 14,000 *g via* Amicon Ultra 4 10-kDa spin filters (EMD Millipore, Billerica, MA, USA) and washed 2 times with 50 mM ammonium bicarbonate to remove soluble components after CS exposure. The remaining material in the filter that was >10 kDa MW was digested overnight with trypsin (20 ng/μl) in 50 mM ammonium bicarbonate at 37°C or chymotrypsin (25 ng/μl) in 100 mM Tris HCl that contained 10 mM $CaCl_2$ at room temperature. The resulting peptide digests were eluted using Amicon Ultra 4 10-kDa spin filters. Peptide mixes were vacuum freeze dried and dissolved in 25 μl of 2% acetonitrile and 0.1% trifluoroacetic acid. Five microliters of solubilized peptide material were injected for proteomic analysis using a Q Exactive (Thermo Fisher Scientific) mass spectrometer coupled to an UltiMate 3000 (Thermo Fisher Scientific) nano-HPLC system. Data acquisition was performed as previously described (34).

Proteomic data analysis

Acquired raw data were processed using Proteome Discoverer 1.4 software (Thermo Fisher Scientific) and searched against the SwissProt protein database (Homo sapiens, November 2016), and the custom sequence of the SPX-101 peptide was searched using the Mascot (Matrix Science, Boston, MA, USA) search engine with parameters set as follows: 5-ppm mass accuracy for parent ions and 0.02-Da accuracy for fragment ions, with 2 missed cleavages allowed. To identify modified peptides of smoke-exposed rSPLUNC1, the Mascpt search algorithm was first set to error-tolerant mode, followed by trypsin- and chymotrypsin-specific searches with variable methionine oxidation, as well as crotonaldehyde and acrolein modification of cysteines. Scaffold 4.7.5 (Proteome Software, Portland, OR, USA) was used to validate tandem mass spectrometry–based peptide and protein identifications. Peptide identifications were accepted if they could be established at >95.0% probability using the Scaffold Local false-discovery rate algorithm. Protein identifications were

accepted if they could be established at >95.0% probability and contained at least two identified peptides. Protein probabilities were assigned using the Protein Prophet algorithm (35).

Circular dichroism

rSPLUNC1 was diluted to 10 μM in PBS buffer loaded into 1-mm cuvettes. Using a Chirascan-Plus instrument (Applied Photophysics, London, United Kingdom), spectra were recorded from 200 to 260 nm at 20 ± 1.0°C as described in Hobbs *et al.* (22). Measurements were corrected for background signal using PBS buffer.

Dynamic light scattering

Dynamic light scattering was used to determine the size of rSPLUNC1 after CS exposure, as previously described (21). Size and ζ potential measurements were conducted using a Zetasizer Nano ZS System (Malvern Instruments, Malvern, United Kingdom). Ten micromolar rSPLUNC1, CS rSPLUNC1, rSPLUNC1^{C180A}, rSPLUNC1^{C224A}, and rSPLUNC1$^{C180/224A}$ were used for size measurements.

β-ENaC mouse studies

All mice used in these studies were on a mixed C57BL/6:C3H background. Airway-specific β-ENaC transgenic (β-ENaC–Tg) mice that overexpressed the Scnn1b gene (24) were obtained from the University of North Carolina Marsico Lung Institute Mouse Model Core. Mice were housed in individually ventilated MV2 Innovive cages in a specific pathogen–free facility maintained at Spyryx Biosciences on a 12-h day/night cycle. Mice were fed a regular chow diet and given water *ad libitum*. Animal E6 protocols were reviewed and approved by the Institutional Animal Care and Use Committee of Spyryx Biosciences.

Data and statistical analysis

The number of replicates performed per experiment is noted in the respective figure legends. All experiments were repeated on ≥3 separate occasions. All experiments conducted using HBECs were repeated using 3–4 different donors on separate occasions with triplicates per donor unless otherwise indicated. Internalization experiments using HEK293T cells were conducted in a multiwell plate on 4 separate occasions with 8 technical replicates per plate. All HBEC mucosal binding and ASL height image analyses were performed using ImageJ software (National Institutes of Health, Bethesda, MD, USA). For HBEC mucosal binding, a histogram plot was generated in ImageJ and data were exported to Prism 7.0 (GraphPad Software, La Jolla, CA, USA). Values that were less than the 25% quartile range were deemed nonspecific binding and thus excluded. Data are shown as means ± SE. Differences between means were tested for statistical significance using Mann-Whitney *U* test, Kruskal-Wallis test with Dunn's multiple comparison test, 2-way ANOVA test with Tukey's multiple comparisons test, and Kaplan-Meier log rank analysis. Statistical analysis was performed using GraphPad Prism 7.0, with values of $P < 0.05$ considered statistically significant.

RESULTS

SPLUNC1 fails to bind to HBEC mucosal surfaces after CS exposure

We have previously demonstrated that rSPLUNC1 binds to HBEC mucosal surfaces *via* interactions with ENaC (20, 21). To test whether CS affected this interaction, we exposed Alexa Fluor 633–labeled rSPLUNC1 to ~13 cigarette puffs of CS or air over 5 min. Air-exposed rSPLUNC1 bound to HBEC mucosal surfaces (**Fig. 1*A, C***); however, CS-exposed rSPLUNC1 failed to bind (Fig 1*B, C*). To confirm that CS exposure did not affect fluorescently labeled rSPLUNC1, *per se*, we examined the fluorescence under cell-free conditions in a multiplate reader. As shown in Fig. 1*D*, CS did not affect the fluorescence of rSPLUNC1-Alexa Fluor 633.

CS prevents SPLUNC1 from regulating ASL height

CS exposure is the main contributor to ASL dehydration as a result of persistent ENaC activity in the absence of functional CFTR (16, 17). As SPLUNC1 is an endogenous negative regulator of ENaC activity, we assessed whether CS impacted the ability of rSPLUNC1 to regulate ENaC-led ASL homeostasis. HBECs were loaded with 20 μl Ringer's solution that contained rhodamine-dextran with 40 μM rSPLUNC1, CS-exposed rSPLUNC1, or Ringer's solution with or without CS as vehicle controls.

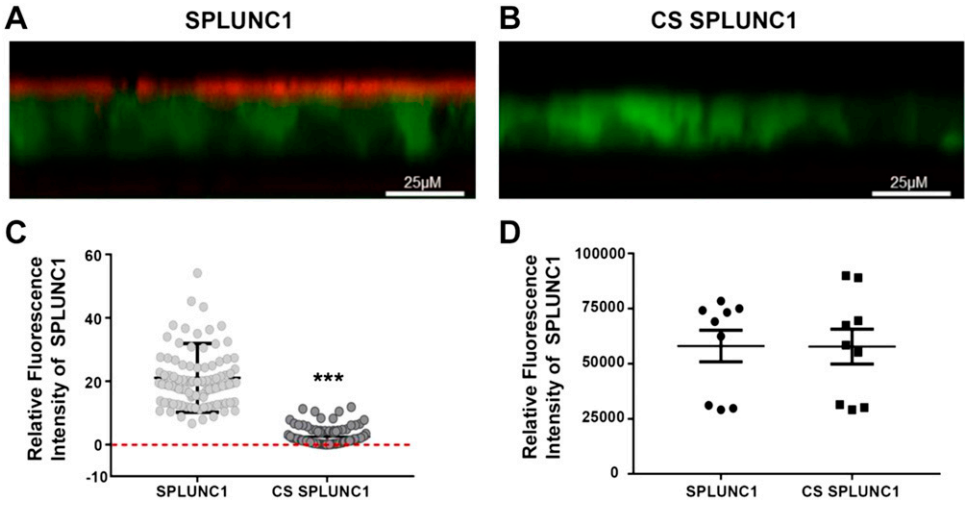

Figure 1. CS inhibits rSPLUNC1 binding to HBEC mucosal surfaces. *A*, *B*) Typical XZ-confocal micrographs of Dylight-labeled rSPLUNC1 with or without CS (red) binding to the mucosal surface of HBECs stained with calcein-AM (green). *C*) Mean data showing relative mucosal binding of Dylight rSPLUNC1 with or without CS to HBECs. Each symbol represents 1 well on the multiwell plate ($n = 9$ from 3 donors). *D*) Control readings for Dylight-labeled SPLUNC1 with or without CS in Ringer's solution in cell-free conditions measured in a multiplate reader ($n = 9$ from 3 donors). ***$P < 0.0001$ (Mann-Whitney *U* test).

CS-Ringer's had no significant effect on ASL height compared with naive Ringer's solution (**Fig. 2*A, B***). Air-exposed rSPLUNC1 significantly increased ASL height after 6 h compared with Ringer's solution with or without CS (Fig. 2*A, B*). Surprisingly, CS-rSPLUNC1 failed to elevate ASL height (Fig. 2*A, B*). To determine whether these effects were reversible, CS-rSPLUNC1 was dialyzed overnight in Ringer's solution. Dialyzed, air-exposed rSPLUNC1 retained its ability to modulate ASL volume; however, dialyzed CS-rSPLUNC1 still failed to regulate ASL volume, which indicates that CS exposure results in irreversible modifications to SPLUNC1 (Fig. 2*C, D*).

CS-SPLUNC1 fails to internalize ENaC

CS-rSPLUNC1 failed to regulate ASL volume, which suggests a failure to regulate ENaC. To test for this, we transiently expressed different combinations of α-, β-, and γ-ENaC subunits in HEK293T cells, with only one subunit tagged per transfection with HA and V5 epitopes at the N and C termini, respectively, as previously described (36). Surface biotinylation followed by Western blot analysis was used to determine the amount of plasma membrane and intracellular ENaC after exposure to 40 μM rSPLUNC1, CS-SPLUNC1, or Ringer's controls. Similar to our previous studies, SPLUNC1 significantly reduced both α-and γ-ENaC subunits at the plasma membrane and in whole-cell lysate (**Fig. 3*A–C***). Consistent with the lack of binding and effect on ASL height (Figs. 1 and 2), CS-rSPLUNC1 failed to internalize α- and γ-ENaC subunits, which indicates that CS blunts the ability of SPLUNC1 to regulate ENaC (Fig. 3*A–C*). As a result of the ability of CS to inhibit SPLUNC1-ENaC internalization in HEK293T cells, we assessed the effect of CS on the ability of SPLUNC1 to regulate ENaC on HBECs.

CS exposure dimerizes and oxidizes SPLUNC1

As we have shown that the ability of rSPLUNC1 to regulate ASL volume and ENaC activity was irreversibly modified after CS exposure, we next used a proteomic approach to look for adduct binding to rSPLUNC1. The

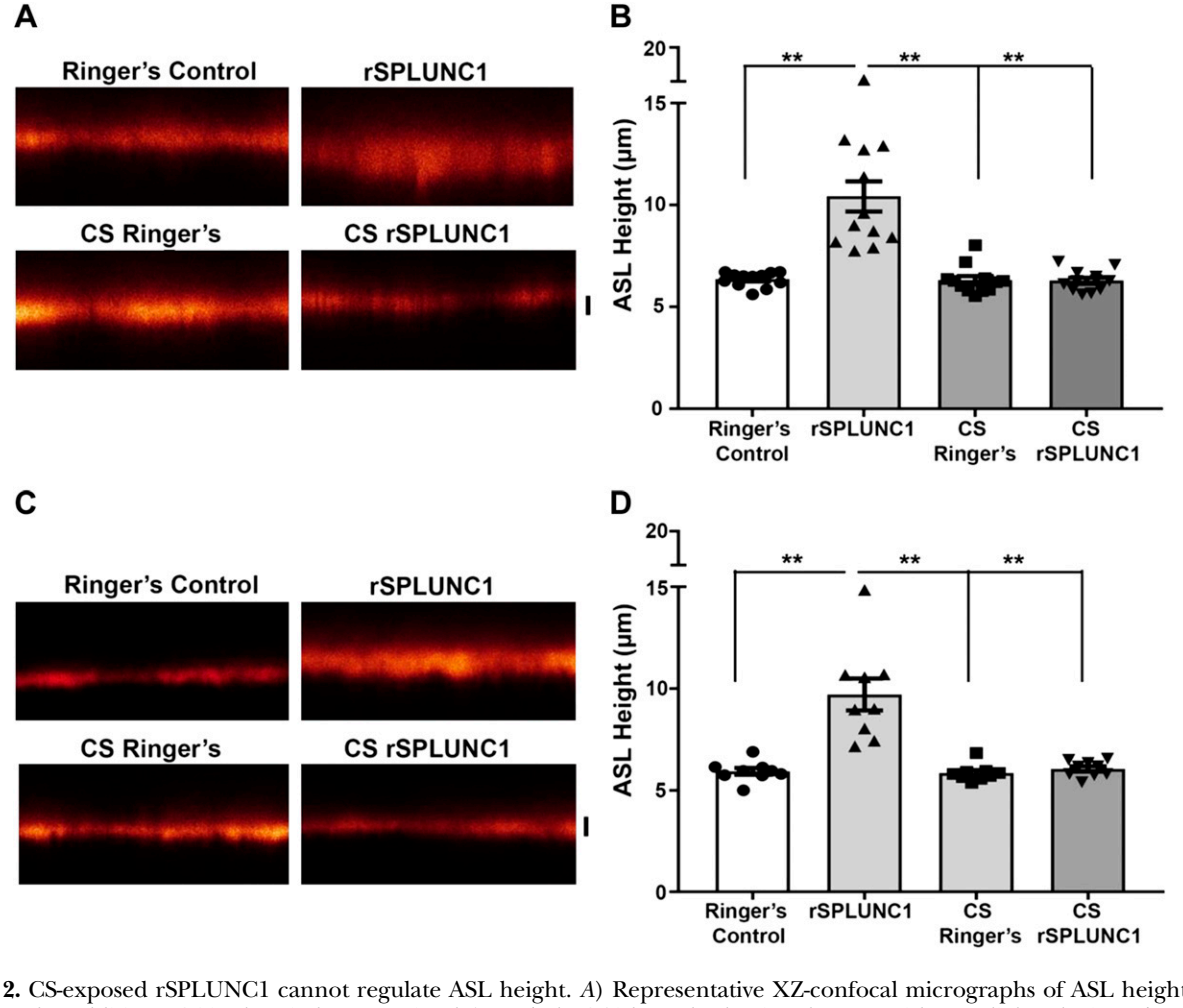

Figure 2. CS-exposed rSPLUNC1 cannot regulate ASL height. *A*) Representative XZ-confocal micrographs of ASL height (red) 6 h after the addition of 20 μl PBS that contained 1 mg/ml of 10-kDa rhodamine-dextran with nondialyzed Ringer's solution (vehicle control), CS-exposed Ringer's solution, or rSPLUNC1 with or without Ringer's solution. *B*) Summary of 6 h ASL height measurements (all: $n = 12$ from 4 donors). *C*) Confocal micrographs of ASL heights after the addition of rSPLUNC1 or CS-exposed rSPLUNC1 that had been dialyzed overnight in Ringer's solution or vehicle controls. *D*) Summary of ASL height measurements of dialyzed samples after 6 h. Each symbol represents 1 transwell [$n = 12$ (*B*) and $n = 9$ (*D*) from 4 and 3 donors, respectively]. Scale bars, 5 μm. Statistically significant differences were measured using Kruskal-Wallis test. $^{**}P < 0.001$.

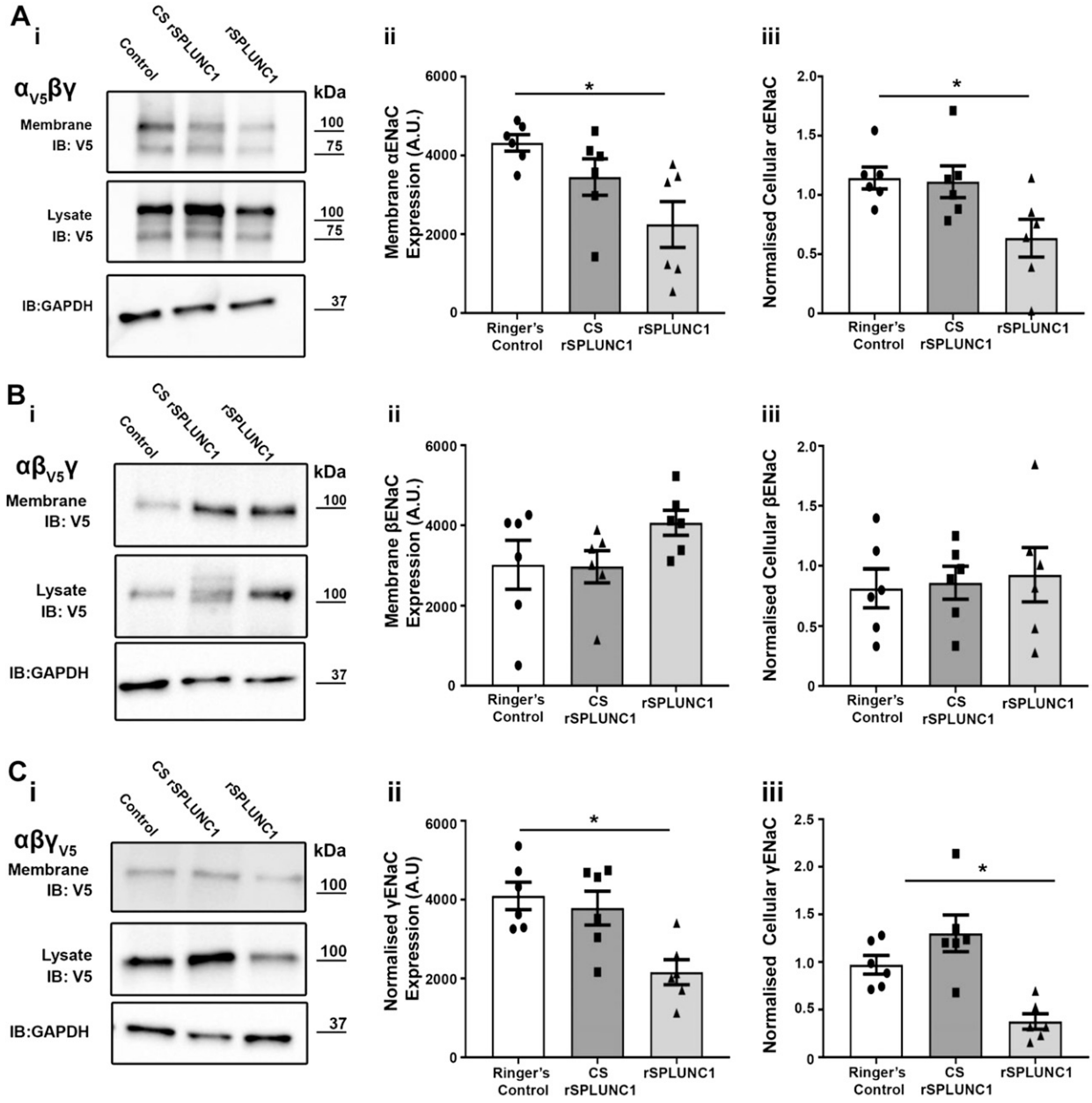

Figure 3. CS-exposed rSPLUNC1 fails to internalize ENaC. HEK293T cells were transiently transfected with ENaC subunits (*i–iii*) as indicated and studied 24 h later. Representative immunoblots and densitometry of membrane and whole-cell protein levels, respectively. α-ENaC (*A*), β-ENaC (*B*), and γ-ENaC (*C*). Whole-cell lysate results are presented as samples normalized to Ringer's control. GAPDH (glyceraldehyde 3-phosphate dehydrogenase) was blotted as a loading control for the lysate. Each symbol represents 1 culture ($n = 6$ from 6 different experiments). *$P < 0.05$ (ANOVA).

crystal structure of human rSPLUNC1 revealed a curved β-sheet flanked by α-helices that together enclose a hydrophobic core (21) (**Fig. 4*A***). rSPLUNC1 also contains 2 cysteine residues at C180 and C224 that may form a disulfide bond (Fig. 4*A*). Using liquid chromatography–tandem mass spectrometry analysis, we detected the majority of SPLUNC1's sequence after tryptic and chymotryptic digestion (211/256 aa, 82% coverage; Fig. 4*B*), including the peptides that encompass the cysteine residues of SPLUNC1. Proteomic analysis further revealed both crotonaldehyde and acrolein modifications to SPLUNC1's 2 cysteine residues (positions 180 and 224; Fig. 4*C–F*). To investigate whether these cysteine modifications were preventable, we preincubated rSPLUNC1 with the antioxidant, glutathione. This maneuver abolished CS-induced modifications of rSPLUNC1 (Fig. 4*G, H*). To determine whether SPLUNC1's MW was altered after CS exposure, we performed SDS-PAGE analysis. Under reducing conditions, an additional band, which was indicative of SPLUNC1 dimerization, was detected after CS exposure by Western blot analysis (Fig. 4*I*). Under native/nonreducing conditions, the shift from monomer to dimer was more pronounced, and the majority of the protein seemed to be dimerized, which indicates that CS structurally alters rSPLUNC1 (Fig. 4*J*).

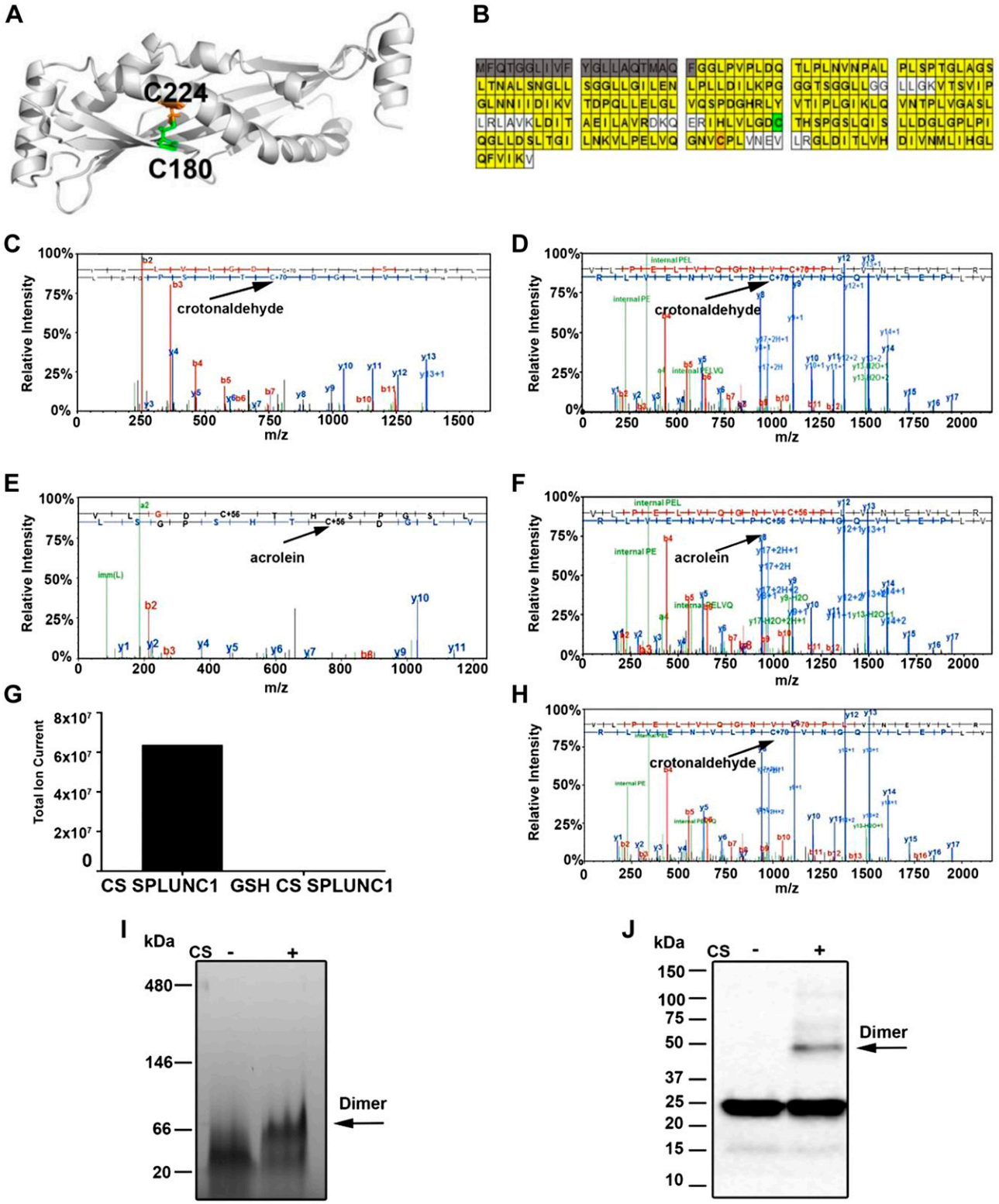

Figure 4. CS induces adduct binding to rSPLUNC1 cysteine residues. *A*) Structure of SPLUNC1, which indicates the positions of cysteine residues C180 (green) and C224 (orange). *B*) rSPLUNC1 coverage as revealed after chymotryptic digestion. Cleaved N-terminal signal sequence is highlighted (gray). Cysteines C180 and C224 are highlighted in green and orange, respectively. *C*, *D*) Representative liquid chromatography–tandem mass spectrometry (LC-MS/MS) spectra showing crotonaldehyde adducts binding to rSPLUNC1's cysteine residues 180 in peptide IHLVLGDCYHSPHSL (*C*) and 224 in peptide VLPELVQGNVCPLV-NEVLR (*D*). *E*, *F*) LC-MS/MS spectra showing acrolein adducts binding to rSPLUNC1's cysteines residue 180 in VLGDCTHSPGSL (*E*) and 224 in peptide VLPELVQGNVCPLVNEVLR (*F*). *G*) Modified peptide was not detected in the presence of 40 μM glutathione. *H*) Total ion current intensity of crotonaldehyde modified SPLUNC1 fragments. *J*) Nonreducing PAGE stained with gel-code blue showing rSPLUNC1 dimer formation with or without CS exposure. *I*) Representative Western blot of rSPLUNC1 with or without CS exposure probed with an anti-SPLUNC1 Ab. Arrows indicate dimers.

SPLUNC1 cysteine residues are critical for ASL volume regulation

Proteomic analysis indicated crotonaldehyde and acrolein binding to rSPLUNC1 cysteines. To assess the impact of these residues on rSPLUNC1 function, we generated the following SPLUNC1 mutants: rSPLUNC1^{C180A}, rSPLUNC1^{C224A}, and rSPLUNC1$^{C180/C224A}$. Both rSPLUNC1^{C180A} and rSPLUNC1^{C224A} retained the ability to regulate ASL height (**Fig. 5*A, B***) and were sensitive to CS exposure (Fig. 5*C–F*). In contrast, rSPLUNC1$^{C180A/C224A}$ failed to regulate ASL height and CS exposure had no additional effect (Fig. 5*G, H*), which suggests that at least 1 cysteine was required for SPLUNC1 activity and that CS binding to both cysteines inhibited function.

Biophysical analysis of the secondary and tertiary structure of CS-exposed SPLUNC1

To determine whether CS alters the secondary structure of SPLUNC1, we performed circular dichroism. Despite CS inducing adduct binding (Fig. 4), there were no significant differences in the spectra of air *vs.* CS-exposed rSPLUNC1 or any of the rSPLUNC1 cysteine mutants (**Fig. 6*A–D***). Similarly, the secondary structure of rSPLUNC1$^{C180A/C224A}$ was unaffected by CS exposure, despite the mutant functionally reprising CS rSPLUNC1. These results indicated that CS-induced cysteine adducts do not affect the secondary structure of SPLUNC1. In contrast to circular dichroism, dynamic light scattering can accurately assess protein oligomerization by determining the hydrodynamic size of each protein. Consistent with our previous study (21), this technique revealed that naive/air-exposed rSPLUNC1 was present as a single peak, which suggests that it predominantly formed monomers; however, the size distribution graph demonstrated that CS-SPLUNC1 was visible as additional peaks between 220 and 400 nm, which indicated aggregation (Fig. 6*E*). In contrast to rSPLUNC1, rSPLUNC1^{C180A} and rSPLUNC1^{C224A} were detected as multiple peaks, which suggests some spontaneous aggregation and, potentially, the formation of intermolecular disulfide bonds, even without CS exposure (Fig. 6*F, G*). Of interest, after CS exposure, these peaks disappeared, which suggests that CS disrupts any intermolecular disulfide bonds that may occur in these mutants. Similar to circular dichroism, rSPLUNC1$^{C180A/C224A}$ contained the same profile in the presence or absence of CS, which suggests that it was incapable of forming αβ-unsaturated aldehyde adducts (Fig. 6*H*).

SPX-101 structure/function is unhindered by CS exposure

We have thus far demonstrated that CS exposure altered the structure and function of rSPLUNC1. Previous reports have shown that SPX-101 can regulate ENaC-led ASL absorption in a dose-dependent manner (23). We exposed SPX-101 to CS and performed proteomic analysis and functional assays. Proteomic analysis indicated that there was no adduct formation to SPX-101 after CS exposure (**Fig. 7*A***). We then treated HBECs with CS-exposed SPX-101 and found that CS-exposed SPX-101 was still able to regulate ASL volume (Fig. 7*B*). Because SPX-101 and CS-SPX-101 were efficacious at regulating ASL volume in HBECs, we assessed the ability of SPX-101 and CS SPX-101 to regulate ENaC activity in HBECs by measuring the amiloride-sensitive transepithelial voltage (V_{tAMIL}). As amiloride can hyperpolarize the apical membrane and induce Cl^- secretion, we pretreated all cultures serosally with bumetanide to inhibit Cl^- uptake. Under baseline conditions, there was an ~8 mV V_{tAMIL}, which suggests that ENaC was active (Fig. 7*C*). SPLUNC1, SPX-101, and CS SPX-101 caused a significant reduction in V_{tAMIL}, which is indicative of attenuation of ENaC activity. In agreement with previous observations, CS-SPLUNC1 failed to attenuate ENaC activity (Fig. 7*C*).

We have previously demonstrated that SPLUNC1 internalizes α-ENaC-GFP, which leads to a quenching of GFP fluorescence in HEK293T cells (37). SPX-101 also induces ENaC internalization (23); therefore, we measured GFP quenching as a marker for internalization using a multiplate reader. Accordingly, we transiently transfected HEK293T cells with α-ENaC-GFP, as well as unlabeled β- and γ-ENaC, and exposed them to SPX-101 with or without CS for 1 h. Both SPX-101 and CS-SPX-101 decreased α-ENaC-GFP fluorescence, which suggests that SPX-101 could still internalize ENaC (Fig. 7*D*). In addition, as a negative control, we expressed GFP-CFTR in HEK293T cells and observed that fluorescence remained unchanged after 1 h of incubation with SPX-101 (Fig. 7*E*). As an additional control, α-ENaC-GFP–transfected HEK293T cells were exposed to CS, and fluorescence intensity remained unchanged compared with Ringer's control (Fig. 7*F*).

To determine whether SPX-101 could help increase ASL hydration in CS-exposed airway epithelia, HBECs were pretreated with SPX-101 or vehicle and exposed to CS or air. Consistent with the *in vivo* phenotype of mucus dehydration and our previous *in vitro* studies (16, 26), ASL height decreased in CS-exposed HBECs; however, with SPX-101 pretreatment, ASL height was maintained in both air- and CS-exposed HBECs compared with vehicle and CS-exposed controls (Fig. 7*G*). As prophylactic SPX-101 treatment prevented CS-induced ASL dehydration, we next assessed whether SPX-101 could also aid in rehydration when added to HBECs. For this, we used HBECs derived from 4 healthy donors and 4 COPD donors. HBECs were exposed to freshly generated CS, and SPX-101 was added apically 1 h after CS exposure. After 30 min with SPX-101, ASL height of CS-exposed cultures was significantly increased greater than normal levels, irrespective of origin, and was not significantly different to ASL height in air-exposed treated SPX-101 cultures (Fig. 7*H*).

β-ENaC-Tg mice overexpress β-ENaC and develop obstructive pulmonary disease broadly similar to COPD (38). SPX-101 has previously been demonstrated to increase the survival of β-ENaC mice when added soon after birth (23). To determine whether CS SPX-101 could have the same effect, β-ENaC mice were treated with 50 mM

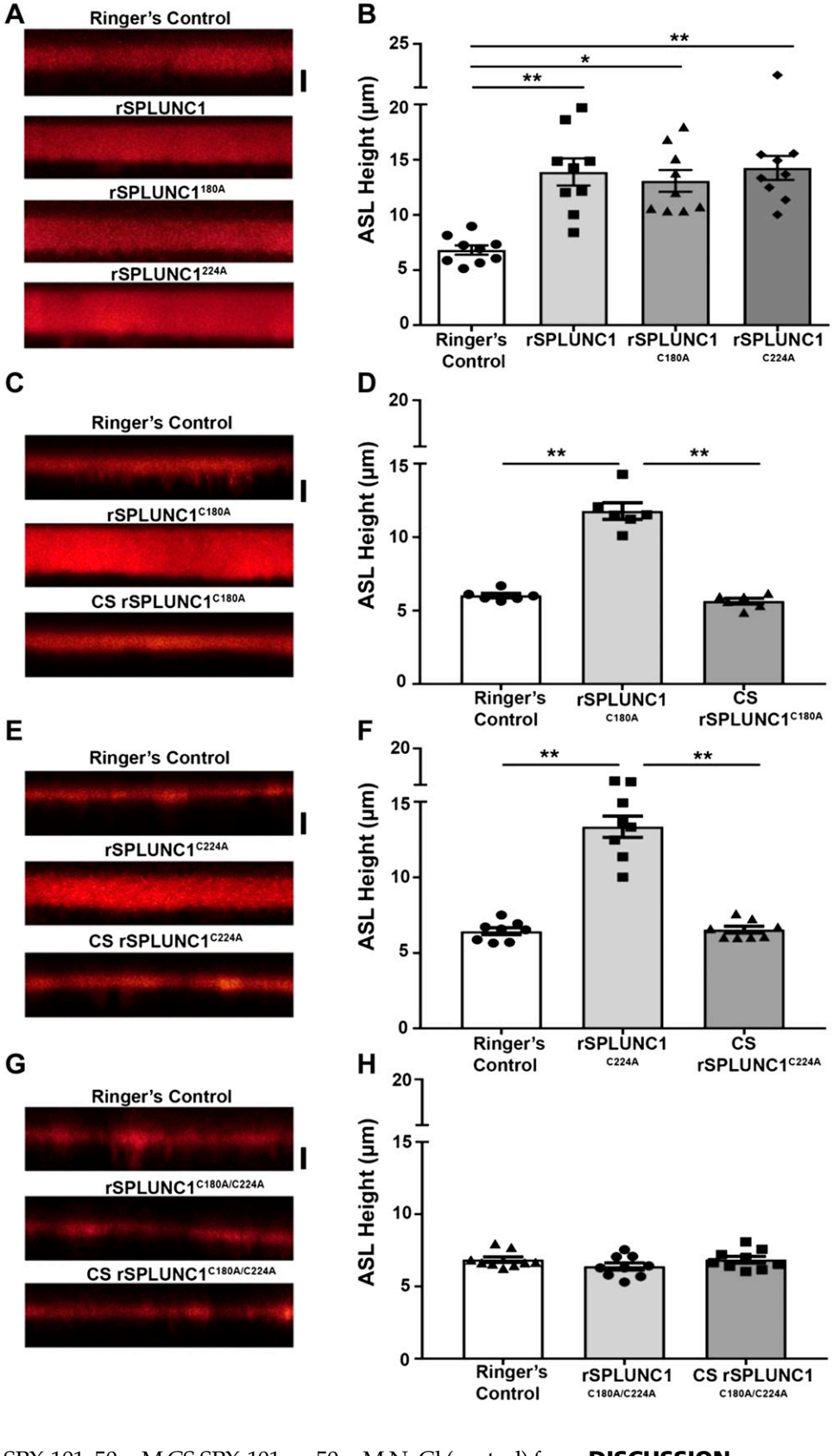

Figure 5. SPLUNC1 cysteine mutants are required for ASL volume homeostasis. *A*, *B*) HBECs were loaded with 20 μl Ringer's solution that contained 1 mg/ml of 10-kDa rhodamine-dextran and 40 μM rSPLUNC1, rSPLUNC1^{C180A}, and rSPLUNC1^{C224A} as indicated, and ASL height was measured by XZ-confocal microscopy (all: $n = 9$ from 3 donors). *C–H*) rSPLUNC1^{C180A} (*C*, *D*), rSPLUNC1^{C224A} (*E*, *F*), and rSPLUNC1$^{C180/C224A}$ (*G*, *H*) were exposed to CS and cultures were subsequently loaded with 40 μM of each protein. Representative XZ confocal micrographs of ASL height (red) 6 h after addition of rSPLUNC1 or rSPLUNC1 mutants (*C*, *E*, *G*), and the mean ASL heights are shown (*D*, *F*, *H*; $n = 9$ from 3 donors). Scale bars, 5 μm. $^*P < 0.01$, $^{**}P < 0.001$ (ANOVA).

SPX-101, 50 mM CS SPX-101, or 50 mM NaCl (control) for up to 14 d. SPX-101 significantly increased the survival rate to 94% with a once-daily intranasal instillation. Similarly, survival with CS-exposed SPX-101 reached 87.5% in mice, which further indicates that CS has no effect on SPX-101 function (Fig. 7*I*).

DISCUSSION

We have previously demonstrated that SPLUNC1 cannot regulate ENaC in acidic cystic fibrosis (CF) ASL (21); however, the impact of CS exposure on the ability of SPLUNC1 to function is less clear. Emerging data indicate

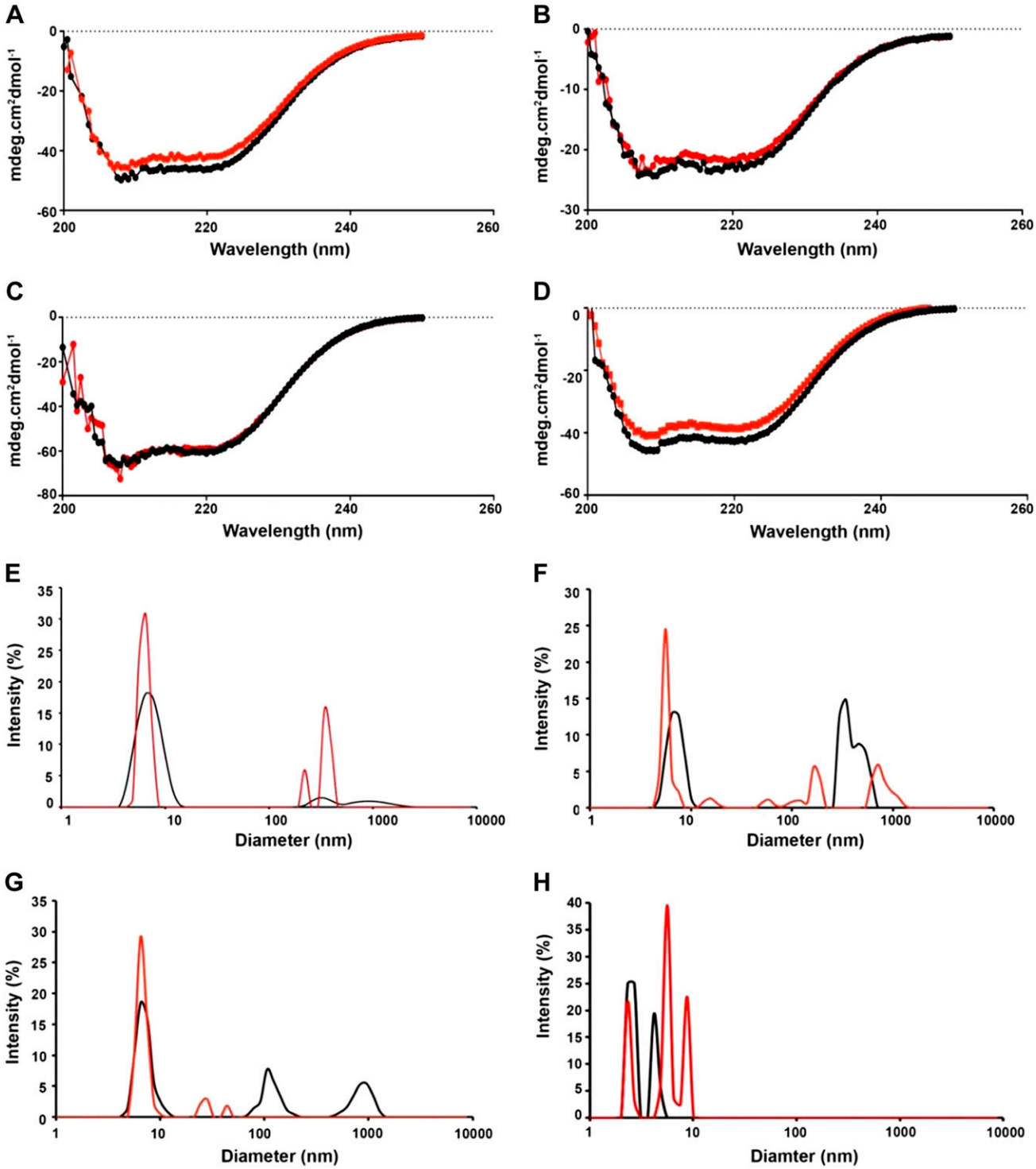

Figure 6. CS-induced aggregation of rSPLUNC1. SPLUNC1 and cysteine mutants were exposed to CS. Structure of rSPLUNC1 (*A*, *E*), rSPLUNC1^{C180A} (*B*, *F*), rSPLUNC1^{C224A} (*C*, *G*), and rSPLUNC1$^{C180A/C224A}$ (*D*, *H*) was analyzed using circular dichroism and dynamic light scattering. All data are representative of 3 individual experiments. Black lines, air-exposed rSPLUNC1; red lines, CS-exposed rSPLUNC1.

that COPD pathogenesis has some similarities with CF. Beyond the chronic neutrophilia, tobacco exposure chronically inhibits CFTR, likely by internalizing CFTR from the plasma membrane, which leads to ASL dehydration (14–16). Whereas CS seems to consistently inhibit CFTR both *in vivo* and *in vitro*, it does not seem to affect ENaC, which suggests that ENaC inhibition is a potential therapy to rebalance ion transport in dehydrated COPD airways. Of importance, our data demonstrate that continued ENaC activity in the absence of CFTR drives this dehydration, and that pretreatment with an ENaC antagonist prevents CS-induced dehydration (17). SPLUNC1 protein levels are reduced in bronchoalveolar lavages from cigarette smokers and patients with COPD compared with

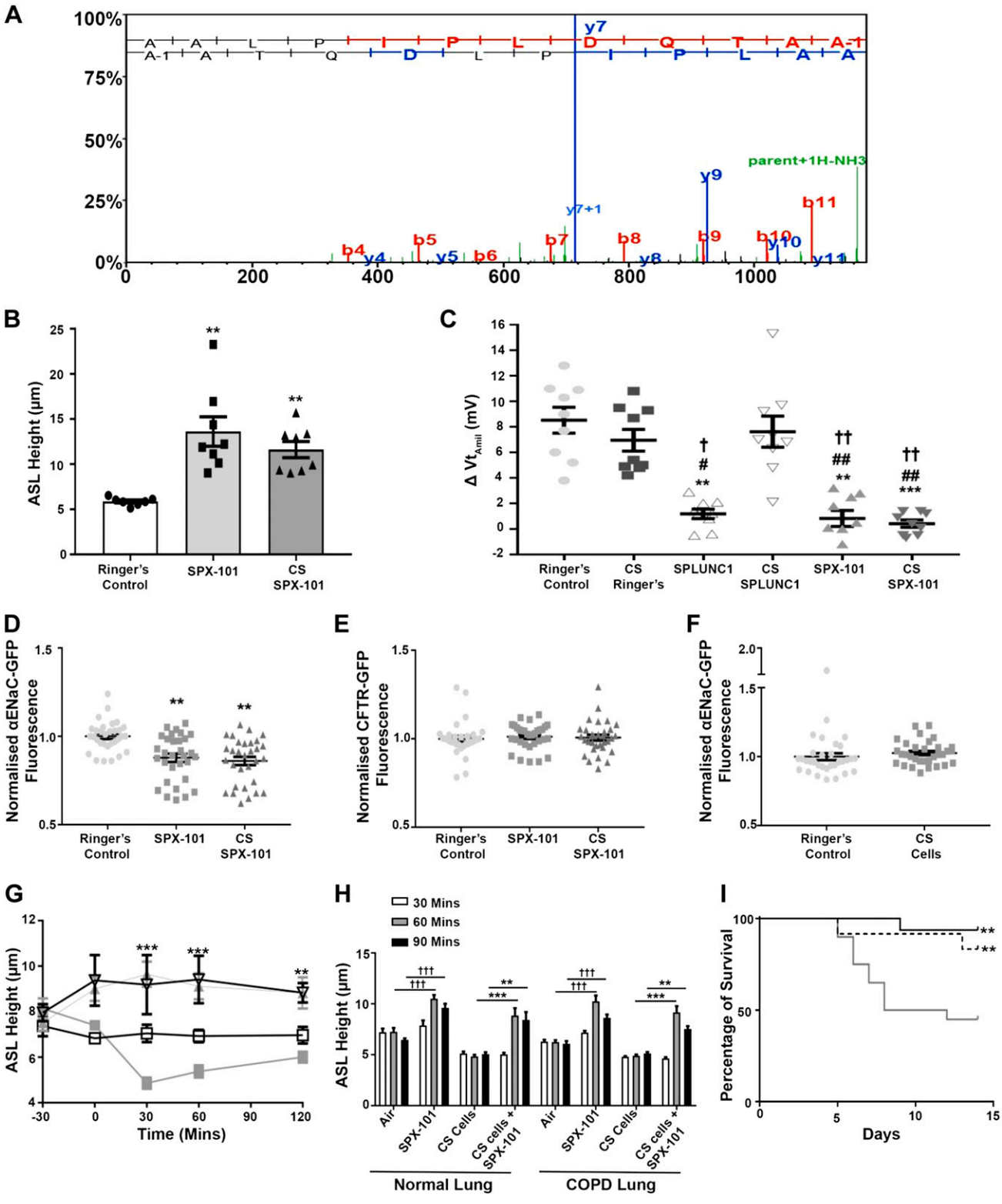

Figure 7. SPX-101 does not bind adducts and remains functional after CS exposure. *A*) Representative liquid chromatography–tandem mass spectrometry spectrum showing CS-exposed SPX-101 peptide, AALPIPLDQTAA. *B*) Summary data of ASL height measurements taken 6 h after mucosal addition of 20 μl Ringer's solution (control) or SPX-101 in Ringer's solution with or without CS exposure (Ringer's, $n = 7$; SPX-101 and CS-SPX-101, $n = 8$). $^{**}P < 0.001$. *C*) Amiloride-sensitive V_ts (V_{tAMIL}) in HBECs after 1 h of exposure to SPLUNC1 or SPX-101 as indicated (all: $n = 9$ from 3 donors). $^{**}P < 0.001$, $^{***}P < 0.0001$ [compared with Ringer's control (ANOVA)], $^{\#}P < 0.01$, $^{\#\#}P < 0.001$ (compared with CS Ringers), $^{\dagger}P < 0.05$, $^{\dagger\dagger}P < 0.001$ (compared with CS Ringers). *D*) Change in fluorescence of α-ENaC transiently transfected in HEK293T cells 3 h after incubation with vehicle or peptide as indicated (all $n = 4$). $^{**}P < 0.001$. *E*) Fluorescence of GFP-CFTR transiently transfected into HEK293T cells after a 3-h exposure to Ringer's solution or SPX-101 with or without CS (all: $n = 4$). *F*) HEK293T cells transfected with α-ENaC-GFP cells

(*continued on next page*)

healthy individuals, which has been attributed to neutrophil elastase–induced degradation (39). However, the direct effects of CS on SPLUNC1 and its subsequent ability to regulate ENaC have not yet been investigated.

Our data indicate that fluorescently labeled rSPLUNC1 failed to bind to HBEC mucosal surfaces after CS exposure (Fig. 1). This was not because of CS-induced quenching of the dye, and rSPLUNC1 remained fluorescent in solution after CS exposure (Fig. 1*D*). As expected, this lack of binding had functional consequences, and after rSPLUNC1 had been exposed to CS, it also failed to regulate ASL homeostasis. In contrast, exposing Ringer's solution to CS, then adding it to cells did not result in ASL dehydration (Fig. 2*A, B*), which is consistent with our previous observation that the components of CS that inhibit CFTR are contained in the volatile phase and not in the water-soluble or tar phases (40). Overnight dialysis in fresh Ringer's solution did not reverse these effects, which suggests that CS irreversibly altered SPLUNC1 and that this was not a result of potential acidification of Ringer's solution by CS exposure (Fig. 2*C, D*). Although the failure to absorb excess ASL after the addition of CS-rSPLUNC1 was most likely a result of ENaC dysregulation (20), this does not prove a direct link between SPLUNC1 and ENaC. We have recently demonstrated that rSPLUNC1 internalized α- and γ-ENaC subunits and targeted them to the lysosome (37); therefore, we assessed whether CS-SPLUNC1 could still internalize α- and γ-ENaC subunits. Similar to ASL height assays, the ability of CS-SPLUNC1 to internalize ENaC and reduce ENaC activity were attenuated after CS exposure (Fig. 3*A–C*), which suggests that SPLUNC1's role as an endogenous inhibitor of ENaC was severely attenuated by CS exposure. HEK293T cells are an immortalized cell line that has enabled us to investigate SPLUNC1-ENaC interactions using transfected wild-type and mutant proteins. For example, we have previously observed that SPLUNC1-induced α- and γ-ENaC internalization occurs in both HEK293T cells and HBECs, which suggests that their use is valid (37). However, as a caveat, although trafficking may be similar between the 2 culture systems, the adaptor/chaperone proteins required may differ.

As the effects of CS were irreversible and resulted in SPLUNC1 aggregation, we next investigated potential chemical modifications to rSPLUNC1 using mass spectrometry. SPLUNC1 contains 2 cysteine residues—C180 and C224—within its β-sheet region (21), and reducing SPLUNC1 with DTT abrogated its ability to inhibit ENaC (19), which suggests that these residues are sensitive to oxidation/reduction. Using an untargeted liquid chromatography–tandem mass spectrometry analysis approach, we identified that the α,β-unsaturated aldehydes, crotonaldehyde and acrolein, bind to both of these residues (Fig. 4*C–F*). Unsurprisingly, the antioxidant, glutathione, prevented CS-induced modifications to SPLUNC1 cysteines (Fig 4). Crotonaldehyde and acrolein are present in micromolar concentrations in CS and exhibit strong reactivity toward cysteine residues (41), which suggests that α,β-unsaturated aldehyde binding to SPLUNC1 may be common in tobacco smokers, and that disruption of the disulfide bonds causes SPLUNC1 dysfunction. These disulfide bonds have not previously been directly studied in the context of SPLUNC1; however, CS exposure to protein-disulfide isomerases results in the nitrosylation of cysteine modifications, which leads to alterations in its 3-dimensional structure (42). Similarly, CS exposure to surfactant protein A also resulted in modifications to cysteine residues (7). However, whether these modifications affected the disulfide bond on surfactant protein A remains to be determined.

As the observed effects of CS on rSPLUNC1 were irreversible (Fig. 2), we performed gel electrophoresis to investigate potential differences in rSPLUNC1's MW. We found that CS caused rSPLUNC1 aggregation under nonreducing conditions and that the majority of SPLUNC1 was dimerized (Fig 4*J*). To investigate whether cysteines play a role in this dimerization, we analyzed control and CS rSPLUNC1 by Western blot under reducing conditions. Here, the majority CS-rSPLUNC1 was present in monomeric form (Fig 4*I*). The minor amount of dimerized CS rSPLUNC1 visible under reduced conditions may have been a result of chemical cross-linking by CS constituents, including acrolein and crotonaldehyde. Because the majority of CS rSPLUNC1 was not cross-linked, these data suggest that the loss of function was related to CS-induced cysteine modifications. We then used biophysical approaches to confirm these observations. Consistent with our electrophoresis experiments (Fig. 4), we observed rSPLUNC1 aggregation after CS exposure by dynamic light scattering for wild-type SPLUNC1 (Fig. 6*E–G*). The molecular radius of rSPLUNC1 was ~6.25 nm; however, after CS exposure, SPLUNC1's radius increased to 250–360 nm, indicating aggregation. On the basis of these data, we propose that CS-induced SPLUNC1 aggregation directly contributes to its failure to regulate ENaC. Although previous reports have demonstrated that CS extract significantly increases ubiquitinated proteins localized in the perinuclear space in Bea2b cells (43), to our knowledge, this is the first report to demonstrate that CS exposure to secreted airway proteins results in aggregation. On the basis of these data, we propose that the ability of SPLUNC1 to regulate ASL volume after CS exposure was a result of SPLUNC1's altered redox state.

were exposed to CS as a control (all: $n = 4$. *G*) HBECs were preloaded with vehicle or peptide, excess ASL was aspirated, cultures were exposed to CS or air as indicated, and ASL height was measured by XZ confocal microscopy. □, air; ■, CS cells; ▽, SPX-101; ▲, CS exposed cells + SPX-101 (all: $n = 9$). $^{**}P < 0.001$, $^{***}P < 0.0001$ (compared with CS cells). *H*) Mean ASL height at time points in HBECs exposed to air or CS followed by SPX-101 where indicated ($n = 12$ from 4 normal donors and $n = 12$ from 4 COPD donors). $^{**}P < 0.001$, $^{***}P < 0.0001$ (compared with CS cells), $^{\dagger\dagger\dagger}P < 0.0001$ (compared with air exposed cells, 2-way ANOVA). *I*) Kaplan-Meier survival curves for β-ENaC mice treated once daily, starting 2 d after birth, with 50 mM SPX-101 ($n = 16$), CS-SPX-101 ($n = 12$), and saline (control, $n = 20$). Solid black line, SPX-101; hashed line, CS SPX-101 solid gray line, saline. $^{**}P < 0.001$ (Wilcoxan match pairs signed rank test, and Kaplan-Meier log-rank analysis).

To better understand the importance of SPLUNC1's disulfide bond, we mutated its cysteines to alanines and used ASL volume homeostasis as a proxy for ENaC regulation. When either cysteine was mutated—rSPLUNC1^{C180A} or rSPLUNC1^{C224A}—normal function and sensitivity to CS exposure remained intact (Fig. 5*A–F*). In contrast, the rSPLUNC1$^{C180A, C224A}$ double mutant lost its ability to regulate ASL volume and was insensitive to CS exposure (Fig. 5*G, H*). A schematic summary of the effect of CS on SPLUNC1 and its cysteine mutants is summarized **Fig. 8**. We propose that under normal conditions, the presence of a disulfide bond between residues C180 and C224 allows rSPLUNC1 to extend its S18 region and potentially interact with ENaC (Fig. 8*A*i). After CS exposure, crotonaldehyde binds to cysteine residues (Fig. 8Aii), disrupting the disulfide bond to possibly cause a conformational change in SPLUNC1 that prevents the S18 region from interacting. Of interest, SPLUNC1^{C180A} was able to retain function (Fig. 5*C, D*). On the basis of our data (Fig 6), we hypothesize that the single cysteine mutants form intermolecular disulfide bonds with adjacent SPLUNC1 molecules to allow the full function of the S18 region (Fig. 8*Bi*); however, these mutants were still sensitive to CS exposure, which attenuated ASL regulation by blocking the disulfide bond formation (Fig. 8*B*). Finally, the double cysteine mutant was inactive and insensitive to CS, which suggests that the missing disulfide bond induces a conformational change that is incompatible with S18 function (Fig. 8*C*).

Although previous reports have demonstrated CS can alter secondary protein structure (42), we found that neither CS exposure, nor cysteine removal altered the relative amounts of rSPLUNC1's α-helix, β-sheet, or disordered regions (Fig. 6*A–C*). SPLUNC1 has a hydrophobic core

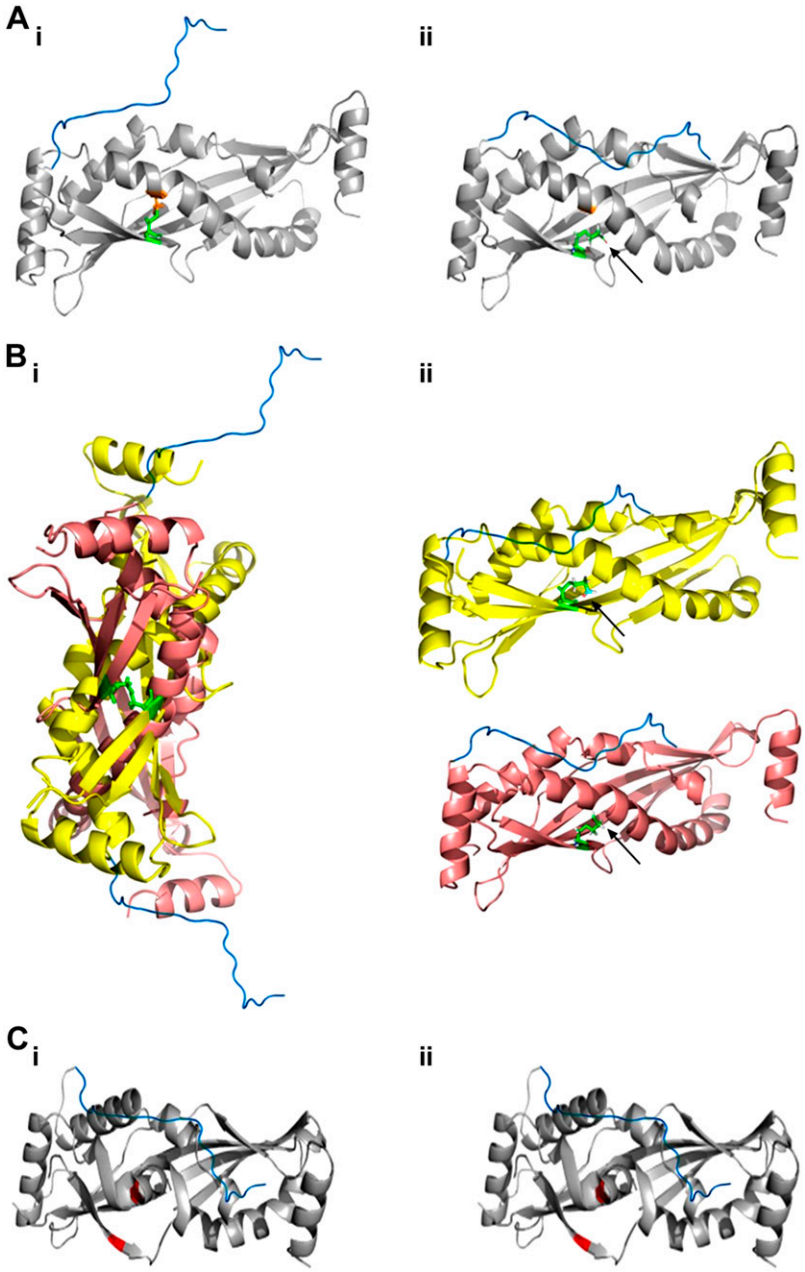

Figure 8. Summary of CS-induced conformational changes to SPLUNC1 structure. SPLUNC1 structure was drawn in Pymol (obtained from Structural Bioinformatics Protein Data Bank, ID: 4KGH). The S18 region (blue; sequence GGLPVPLDQTLPLNVNPA) was manually docked onto residue S43. Cysteines 180 and 224 are shown in orange and green, respectively. *Ai*) Wild-type (WT) SPLUNC1 with the outstretched S18 region. *Aii*) CS-exposed WT SPLUNC1, with crotonaldehyde binding indicated (arrow), leading to a conformational change in the S18 region. *Bi*) SPLUNC1^{C180A} retains the ability to regulate ENaC by forming intermolecular disulfide bonds with adjacent SPLUNC1^{C180A}. *Bii*) CS-exposed SPLUNC1^{C180A} renders function inactive with the separation of the 2 molecules. *Ci*) SPLUNC1$^{C180/C224A}$ regulatory function is attenuated to conformational change of structure and the S18 region. *Cii*) CS had no additional effect on SPLUNC1$^{C180/C224A}$ function.

usually shielded by other residues. Indeed, SPLUNC1 has been described as both a super role protein that can unfold at the air-liquid interface to reduce surface tension (44) and as a tubular lipid-binding protein that uses its hydrophobic core to bind lipids (45). Thus, we speculate that ablation of the disulfide bond exposes the hydrophobic core, which leads to aggregation. Despite the lack of a cysteine residue, single mutants could still regulate ASL height (Fig. 5), and we observed spontaneous dimerization, even in the absence of CS exposure (Fig. 6*F*, *G*). These data suggest that, in the absence of 1 cysteine, SPLUNC1 may form intramolecular disulfide bonds that serve to stabilize the molecule and allow it to perform its normal functions. Of interest, rSPLUNC1$^{C180A, C224A}$ spontaneously aggregated and no additional aggregation occurred after CS exposure (Fig. 6*H*). On the basis of these data, we propose that CS-induced SPLUNC1 aggregation after α,β-unsaturated aldehyde binding to the 2 cysteines directly contributes to its failure to regulate ENaC.

Acrolein and crotonaldehyde are major constituents of CS that are responsible for cysteine adduct binding, the release of IL-8 in human macrophage cell lines, and the inhibition of the production of several proinflammatory cytokines, including IL-2 and TNF-α (2, 46–48). Glutathione is an important antioxidant present in the ASL (49), and α,β-unsaturated aldehyde exposure decreases glutathione levels, thereby increasing the formation of reactive oxygen species (3, 50). As the progression of COPD is associated with increased oxidative stress (51, 52) and reduced antioxidants (50), loss of SPLUNC1 function may be more pronounced as COPD worsens. Detection of adducts on SPLUNC1 and other proteins in the airways of tobacco users and patients with COPD may serve as novel biomarkers of exposure/harm that can be used to assess the toxicity of different tobacco products. Indeed, as a biomarker, adduct formation may have increased sensitivity as it does not require changes in protein expression to be quantified.

SPX-101 is currently being evaluated as a therapeutic for the treatment of ASL dehydration/mucus stasis in CF (23). As SPX-101 does not have cysteines, and because CS/COPD airways are also characterized by ASL/mucus dehydration (53, 54), we tested the hypothesis that SPX-101 could treat mucus dehydration in CS-exposed airway cultures. Whereas some patients with COPD stop smoking after diagnosis, many continue, which suggests that air-inhaled therapy will need to be smoke proof (54). Indeed, we were unable to detect adduct binding to SPX-101 after CS exposure, which suggests that it may be useful in this context (Fig. 7*A*). Similarly, CS-exposed SPX-101 was still able to regulate ASL height. As an indicator of ENaC activity, we measured the amiloride-sensitive voltage (V_{tAMIL}) across HBECs after mucosal incubation with SPLUNC1 or SPX-101. As predicted, CS exposure abolished the ability of SPLUNC1 to inhibit V_{tAMIL}. In contrast, SPX-101 remained CS independent and was able to significantly attenuate ENaC activity under these thin film conditions (Fig. 7). In addition, both SPX-101 and CS SPX-101 were able to internalize α-ENaC, but not CFTR, which suggests that it is unaffected by CS exposure (Fig. 7). Furthermore, when added after CS had decreased ASL volume, SPX-101 was still able to increase ASL hydration (Fig. 7). Finally, to demonstrate that CS-exposed SPX-101 works *in vivo*, we used a Tg mouse model in which β-ENaC was overexpressed, leading to spontaneous CF/COPD-like lung disease and a 50% mortality rate (24). Consistent with HBEC experiments, CS-exposed SPX-101 significantly increased β-ENaC mouse survival when added to lungs *via* intranasal delivery. Taken together, these data indicate that SPX-101 may be useful as a treatment for chronic smokers and patients with COPD. An advantage of using intrinsically disordered peptides, such as SPX-101, is that they achieve a greater contact area with their target protein, thus maximizing binding efficiency (56). Furthermore, there is no reason why it cannot be used in conjunction with existing COPD therapies, such as bronchodilators, to yield favorable results.

In summary, we have demonstrated by functional assay and using proteomic approaches that SPLUNC1 structure and function are irreversibly modified by α,β-unsaturated aldehydes present in CS. Because mucus/ASL dehydration is a component of COPD pathogenesis, our results suggest that aldehyde modification of SPLUNC1 is a key event in the dysregulation of ASL volume homeostasis. The presence of dysfunctional SPLUNC1 in the COPD lung is overcome by SPX-101, and our results suggest that SPX-101 could be used as therapy for patients with COPD who have dehydrated ASL/mucus. FJ

ACKNOWLEDGMENTS

The authors thank the University of North Carolina CF Center Tissue Core for providing cells, Rodney Gilmore (University of North Carolina, Chapel Hill) for generating constructs, Dr. Colin Bingle (University of Sheffield, Sheffield, United Kingdom) for providing the full length SPLUNC1 construct, Dr. Michael Miley and Richard Feng (University of North Carolina) for purifying SPLUNC1 and SPLUNC1 cysteine mutants, Prof. Deborah Baines (St. George's University, London, United Kingdom) for providing the αENaC-GFP construct, Dr. Bruce Stanton (Dartmouth College, Hanover, NH, USA) for providing the CFTR-GFP construct, and Dr. Brian Kuhlmann (University of North Carolina) for assistance with circular dichroism. This study was funded by Spyryx Biosciences, U.S. National Institutes of Health (NIH) National Institute of Diabetes and Digestive and Kidney Diseases Grant P30DK065988, NIH National Heart, Lung, and Blood Institute Grant HL135642 and HL103940, and Cystic Fibrosis Foundation Grant R026-CR11. R.T. is a founder of and has equity in Spyryx Bioscience. J.S. is an employee of and has equity in Spyryx Bioscience. The authors declare no conflicts of interest.

AUTHOR CONTRIBUTIONS

P. J. Moore, B. Reidel, J. Sesma, A. Ghosh, M. Kesimer, and R. Tarran designed experiments, performed research, and analyzed data; P. J. Moore, B. Reidel, and R. Tarran wrote the manuscript; and all authors reviewed and approved the manuscript.

REFERENCES

1. Talhout, R., Schulz, T., Florek, E., van Benthem, J., Wester, P., and Opperhuizen, A. (2011) Hazardous compounds in tobacco smoke. *Int. J. Environ. Res. Public Health* **8**, 613–628

2. Witschi, H. (2005) Carcinogenic activity of cigarette smoke gas phase and its modulation by beta-carotene and N-acetylcysteine. *Toxicol. Sci.* **84**, 81–87
3. Facchinetti, F., Amadei, F., Geppetti, P., Tarantini, F., Di Serio, C., Dragotto, A., Gigli, P. M., Catinella, S., Civelli, M., and Patacchini, R. (2007) α,β-Unsaturated aldehydes in cigarette smoke release inflammatory mediators from human macrophages. *Am. J. Respir. Cell Mol. Biol.* **37**, 617–623
4. Ichihashi, K., Osawa, T., Toyokuni, S., and Uchida, K. (2001) Endogenous formation of protein adducts with carcinogenic aldehydes: implications for oxidative stress. *J. Biol. Chem.* **276**, 23903–23913
5. Drost, E. M., Skwarski, K. M., Sauleda, J., Soler, N., Roca, J., Agusti, A., and MacNee, W. (2005) Oxidative stress and airway inflammation in severe exacerbations of COPD. *Thorax* **60**, 293–300
6. Lärstad, M., Almstrand, A.-C., Larsson, P., Bake, B., Larsson, S., Ljungström, E., Mirgorodskaya, E., and Olin, A.-C. (2015) Surfactant protein A in exhaled endogenous particles is decreased in chronic obstructive pulmonary disease (COPD) patients: A pilot study. *PLoS One* **10**, e0144463
7. Takamiya, R., Uchida, K., Shibata, T., Maeno, T., Kato, M., Yamaguchi, Y., Ariki, S., Hasegawa, Y., Saito, A., Miwa, S., Takahashi, H., Akaike, T., Kuroki, Y., and Takahashi, M. (2017) Disruption of the structural and functional features of surfactant protein A by acrolein in cigarette smoke. *Sci. Rep.* **7**, 8304
8. Kirkham, P. A., Spooner, G., Rahman, I., and Rossi, A. G. (2004) Macrophage phagocytosis of apoptotic neutrophils is compromised by matrix proteins modified by cigarette smoke and lipid peroxidation products. *Biochem. Biophys. Res. Commun.* **318**, 32–37
9. Tran, T. N., Kosaraju, M. G., Tamamizu-Kato, S., Akintunde, O., Zheng, Y., Bielicki, J. K., Pinkerton, K., Uchida, K., Lee, Y. Y., and Narayanaswami, V. (2014) Acrolein modification impairs key functional features of rat apolipoprotein E: identification of modified sites by mass spectrometry. *Biochemistry* **53**, 361–375
10. Lozano, R., Naghavi, M., Foreman, K., Lim, S., Shibuya, K., Aboyans, V., Abraham, J., Adair, T., Aggarwal, R., Ahn, S. Y., Alvarado, M., Anderson, H. R., Anderson, L. M., Andrews, K. G., Atkinson, C., Baddour, L. M., Barker-Collo, S., Bartels, D. H., Bell, M. L., Benjamin, E. J., Bennett, D., Bhalla, K., Bikbov, B., Bin Abdulhak, A., Birbeck, G., Blyth, F., Bolliger, I., Boufous, S., Bucello, C., Burch, M., Burney, P., Carapetis, J., Chen, H., Chou, D., Chugh, S. S., Coffeng, L. E., Colan, S. D., Colquhoun, S., Colson, K. E., Condon, J., Connor, M. D., Cooper, L. T., Corriere, M., Cortinovis, M., de Vaccaro, K. C., Couser, W., Cowie, B. C., Criqui, M. H., Cross, M., Dabhadkar, K. C., Dahodwala, N., De Leo, D., Degenhardt, L., Delossantos, A., Denenberg, J., Des Jarlais, D. C., Dharmaratne, S. D., Dorsey, E. R., Driscoll, T., Duber, H., Ebel, B., Erwin, P. J., Espindola, P., Ezzati, M., Feigin, V., Flaxman, A. D., Forouzanfar, M. H., Fowkes, F. G., Franklin, R., Fransen, M., Freeman, M. K., Gabriel, S. E., Gakidou, E., Gaspari, F., Gillum, R. F., Gonzalez-Medina, D., Halasa, Y. A., Haring, D., Harrison, J. E., Havmoeller, R., Hay, R. J., Hoen, B., Hotez, P. J., Hoy, D., Jacobsen, K. H., James, S. L., Jasrasaria, R., Jayaraman, S., Johns, N., Karthikeyan, G., Kassebaum, N., Keren, A., Khoo, J. P., Knowlton, L. M., Kobusingye, O., Koranteng, A., Krishnamurthi, R., Lipnick, M., Lipshultz, S. E., Ohno, S. L., Mabweijano, J., MacIntyre, M. F., Mallinger, L., March, L., Marks, G. B., Marks, R., Matsumori, A., Matzopoulos, R., Mayosi, B. M., McAnulty, J. H., McDermott, M. M., McGrath, J., Mensah, G. A., Merriman, T. R., Michaud, C., Miller, M., Miller, T. R., Mock, C., Mocumbi, A. O., Mokdad, A. A., Moran, A., Mulholland, K., Nair, M. N., Naldi, L., Narayan, K. M., Nasseri, K., Norman, P., O'Donnell, M., Omer, S. B., Ortblad, K., Osborne, R., Ozgediz, D., Pahari, B., Pandian, J. D., Rivero, A. P., Padilla, R. P., Perez-Ruiz, F., Perico, N., Phillips, D., Pierce, K., Pope III, C. A., Porrini, E., Pourmalek, F., Raju, M., Ranganathan, D., Rehm, J. T., Rein, D. B., Remuzzi, G., Rivara, F. P., Roberts, T., De León, F. R., Rosenfeld, L. C., Rushton, L., Sacco, R. L., Salomon, J. A., Sampson, U., Sanman, E., Schwebel, D. C., Segui-Gomez, M., Shepard, D. S., Singh, D., Singleton, J., Sliwa, K., Smith, E., Steer, A., Taylor, J. A., Thomas, B., Tleyjeh, I. M., Towbin, J. A., Truelsen, T., Undurraga, E. A., Venketasubramanian, N., Vijayakumar, L., Vos, T., Wagner, G. R., Wang, M., Wang, W., Watt, K., Weinstock, M. A., Weintraub, R., Wilkinson, J. D., Woolf, A. D., Wulf, S., Yeh, P. H., Yip, P., Zabetian, A., Zheng, Z. J., Lopez, A. D., Murray, C. J., AlMazroa, M. A., and Memish, Z. A. (2012) Global and regional mortality from 235 causes of death for 20 age groups in 1990 and 2010: a systematic analysis for the Global Burden of Disease Study 2010. *Lancet* **380**, 2095–2128
11. Hirota, N., and Martin, J. G. (2013) Mechanisms of airway remodeling. *Chest* **144**, 1026–1032
12. Hogg, J. C., and Timens, W. (2009) The pathology of chronic obstructive pulmonary disease. *Annu. Rev. Pathol.* **4**, 435–459
13. Tarran, R., Grubb, B. R., Gatzy, J. T., Davis, C. W., and Boucher, R. C. (2001) The relative roles of passive surface forces and active ion transport in the modulation of airway surface liquid volume and composition. *J. Gen. Physiol.* **118**, 223–236
14. Kreindler, J. L., Jackson, A. D., Kemp, P. A., Bridges, R. J., and Danahay, H. (2005) Inhibition of chloride secretion in human bronchial epithelial cells by cigarette smoke extract. *Am. J. Physiol. Lung Cell. Mol. Physiol.* **288**, L894–L902
15. Raju, S. V., Jackson, P. L., Courville, C. A., McNicholas, C. M., Sloane, P. A., Sabbatini, G., Tidwell, S., Tang, L. P., Liu, B., Fortenberry, J. A., Jones, C. W., Boydston, J. A., Clancy, J. P., Bowen, L. E., Accurso, F. J., Blalock, J. E., Dransfield, M. T., and Rowe, S. M. (2013) Cigarette smoke induces systemic defects in cystic fibrosis transmembrane conductance regulator function. *Am. J. Respir. Crit. Care Med.* **188**, 1321–1330
16. Clunes, L. A., Davies, C. M., Coakley, R. D., Aleksandrov, A. A., Henderson, A. G., Zeman, K. L., Worthington, E. N., Gentzsch, M., Kreda, S. M., Cholon, D., Bennett, W. D., Riordan, J. R., Boucher, R. C., and Tarran, R. (2012) Cigarette smoke exposure induces CFTR internalization and insolubility, leading to airway surface liquid dehydration. *FASEB J.* **26**, 533–545
17. Åstrand, A. B. M., Hemmerling, M., Root, J., Wingren, C., Pesic, J., Johansson, E., Garland, A. L., Ghosh, A., and Tarran, R. (2015) Linking increased airway hydration, ciliary beating, and mucociliary clearance through ENaC inhibition. *Am. J. Physiol. Lung Cell. Mol. Physiol.* **308**, L22–L32
18. Anderson, W. H., Coakley, R. D., Button, B., Henderson, A. G., Zeman, K. L., Alexis, N. E., Peden, D. B., Lazarowski, E. R., Davis, C. W., Bailey, S., Fuller, F., Almond, M., Qaqish, B., Bordonali, E., Rubinstein, M., Bennett, W. D., Kesimer, M., and Boucher, R. C. (2015) The relationship of mucus concentration (hydration) to mucus osmotic pressure and transport in chronic bronchitis. *Am. J. Respir. Crit. Care Med.* **192**, 182–190
19. Matalon, S., Bartoszewski, R., and Collawn, J. F. (2015) Role of epithelial sodium channels in the regulation of lung fluid homeostasis. *Am. J. Physiol. Lung Cell. Mol. Physiol.* **309**, L1229–L1238
20. Garcia-Caballero, A., Rasmussen, J. E., Gaillard, E., Watson, M. J., Olsen, J. C., Donaldson, S. H., Stutts, M. J., and Tarran, R. (2009) SPLUNC1 regulates airway surface liquid volume by protecting ENaC from proteolytic cleavage. *Proc. Natl. Acad. Sci. USA* **106**, 11412–11417
21. Garland, A. L., Walton, W. G., Coakley, R. D., Tan, C. D., Gilmore, R. C., Hobbs, C. A., Tripathy, A., Clunes, L. A., Bencharit, S., Stutts, M. J., Betts, L., Redinbo, M. R., and Tarran, R. (2013) Molecular basis for pH-dependent mucosal dehydration in cystic fibrosis airways. *Proc. Natl. Acad. Sci. USA* **110**, 15973–15978
22. Hobbs, C. A., Blanchard, M. G., Alijevic, O., Tan, C. D., Kellenberger, S., Bencharit, S., Cao, R., Kesimer, M., Walton, W. G., Henderson, A. G., Redinbo, M. R., Stutts, M. J., and Tarran, R. (2013) Identification of the SPLUNC1 ENaC-inhibitory domain yields novel strategies to treat sodium hyperabsorption in cystic fibrosis airway epithelial cultures. *Am. J. Physiol. Lung Cell. Mol. Physiol.* **305**, L990–L1001
23. Scott, D. W., Walker, M. P., Sesma, J., Wu, B., Stuhlmiller, T. J., Sabater, J. R., Abraham, W. M., Crowder, T. M., Christensen, D. J., and Tarran, R. (2017) SPX-101 is a novel ENaC-targeted therapeutic for cystic fibrosis that restores mucus transport. *Am. J. Respir. Crit. Care Med.* **196**, 734–744
24. Mall, M., Grubb, B. R., Harkema, J. R., O'Neal, W. K., and Boucher, R. C. (2004) Increased airway epithelial Na^+ absorption produces cystic fibrosis-like lung disease in mice. *Nat. Med.* **10**, 487–493
25. Clunes, L. A., Bridges, A., Alexis, N., and Tarran, R. (2008) *In vivo* versus *in vitro* airway surface liquid nicotine levels following cigarette smoke exposure. *J. Anal. Toxicol.* **32**, 201–207
26. Tyrrell, J., Qian, X., Freire, J., and Tarran, R. (2015) Roflumilast combined with adenosine increases mucosal hydration in human airway epithelial cultures after cigarette smoke exposure. *Am. J. Physiol. Lung Cell. Mol. Physiol.* **308**, L1068–L1077
27. Tarran, R., Trout, L., Donaldson, S. H., and Boucher, R. C. (2006) Soluble mediators, not cilia, determine airway surface liquid volume in normal and cystic fibrosis superficial airway epithelia. *J. Gen. Physiol.* **127**, 591–604
28. Randell, S. H., Fulcher, M. L., O'Neal, W., and Olsen, J. C. (2011) Primary epithelial cell models for cystic fibrosis research. In *Cystic*

Fibrosis: Diagnosis and Protocols, Volume II: Methods and Resources to Understand Cystic Fibrosis (Amaral, M. D., and Kunzelmann, K., eds.), pp. 285–310, Humana Press, Totowa, NJ, USA
29. Hobbs, C. A., Blanchard, M. G., Alijevic, O., Tan, C. D., Kellenberger, S., Bencharit, S., Cao, R., Kesimer, M., Walton, W. G., Henderson, A. G., Redinbo, M. R., Stutts, M. J., and Tarran, R. (2013) Identification of SPLUNC1's ENaC-inhibitory domain yields novel strategies to treat sodium hyperabsorption in cystic fibrosis airway cultures. *Am. J. Physiol. Lung Cell Mol. Physiol.* **305**, L990–L1001
30. Hughey, R. P., Mueller, G. M., Bruns, J. B., Kinlough, C. L., Poland, P. A., Harkleroad, K. L., Carattino, M. D., and Kleyman, T. R. (2003) Maturation of the epithelial Na^+ channel involves proteolytic processing of the alpha- and gamma-subunits. *J. Biol. Chem.* **278**, 37073–37082
31. Woollhead, A. M., and Baines, D. L. (2006) Forskolin-induced cell shrinkage and apical translocation of functional enhanced green fluorescent protein-human alphaENaC in H441 lung epithelial cell monolayers. *J. Biol. Chem.* **281**, 5158–5168
32. Moyer, B. D., Denton, J., Karlson, K. H., Reynolds, D., Wang, S., Mickle, J. E., Milewski, M., Cutting, G. R., Guggino, W. B., Li, M., and Stanton, B. A. (1999) A PDZ-interacting domain in CFTR is an apical membrane polarization signal. *J. Clin. Invest.* **104**, 1353–1361
33. Wiśniewski, J. R., Zougman, A., Nagaraj, N., and Mann, M. (2009) Universal sample preparation method for proteome analysis. *Nat. Methods* **6**, 359–362
34. Kesimer, M., Cullen, J., Cao, R., Radicioni, G., Mathews, K. G., Seiler, G., and Gookin, J. L. (2015) Excess secretion of gel-forming mucins and associated innate defense proteins with defective mucin unpackaging underpin gallbladder mucocele formation in dogs. *PLoS One* **10**, e0138988
35. Nesvizhskii, A. I., Keller, A., Kolker, E., and Aebersold, R. (2003) A statistical model for identifying proteins by tandem mass spectrometry. *Anal. Chem.* **75**, 4646–4658
36. Hobbs, C. A., Da Tan, C., and Tarran, R. (2013) Does epithelial sodium channel hyperactivity contribute to cystic fibrosis lung disease? *J. Physiol.* **591**, 4377–4387
37. Kim, C. S., Ahmad, S., Wu, T., Walton, W. G., Redinbo, M. R., and Tarran, R. (2018) SPLUNC1 is an allosteric modulator of the epithelial sodium channel. *FASEB J.* **32**, 2478–2491
38. Zhou-Suckow, Z., Duerr, J., Hagner, M., Agrawal, R., and Mall, M. A. (2017) Airway mucus, inflammation and remodeling: emerging links in the pathogenesis of chronic lung diseases. *Cell Tissue Res.* **367**, 537–550
39. Jiang, D., Wenzel, S. E., Wu, Q., Bowler, R. P., Schnell, C., and Chu, H. W. (2013) Human neutrophil elastase degrades SPLUNC1 and impairs airway epithelial defense against bacteria. *PLoS One* **8**, e64689
40. Rasmussen, J. E., Sheridan, J. T., Polk, W., Davies, C. M., and Tarran, R. (2014) Cigarette smoke-induced Ca^{2+} release leads to cystic fibrosis transmembrane conductance regulator (CFTR) dysfunction. *J. Biol. Chem.* **289**, 7671–7681
41. Lambert, C., Li, J., Jonscher, K., Yang, T.-C., Reigan, P., Quintana, M., Harvey, J., and Freed, B. M. (2007) Acrolein inhibits cytokine gene expression by alkylating cysteine and arginine residues in the NF-kappaB1 DNA binding domain. *J. Biol. Chem.* **282**, 19666–19675
42. Kenche, H., Ye, Z.-W., Vedagiri, K., Richards, D. M., Gao, X.-H., Tew, K. D., Townsend, D. M., and Blumental-Perry, A. (2016) Adverse outcomes associated with cigarette smoke radicals related to damage to protein-disulfide isomerase. *J. Biol. Chem.* **291**, 4763–4778
43. Tran, I., Ji, C., Ni, I., Min, T., Tang, D., and Vij, N. (2015) Role of cigarette smoke-induced aggresome formation in chronic obstructive pulmonary disease-emphysema pathogenesis. *Am. J. Respir. Cell Mol. Biol.* **53**, 159–173
44. Walton, W. G., Ahmad, S., Little, M. S., Kim, C. S. K., Tyrrell, J., Lin, Q., Di, Y. P., Tarran, R., and Redinbo, M. R. (2016) Structural features essential to the antimicrobial functions of human SPLUNC1. *Biochemistry* **55**, 2979–2991
45. Wong, L. H., and Levine, T. P. (2017) Tubular lipid binding proteins (TULIPs) growing everywhere. *Biochim. Biophys. Acta* **1864**, 1439–1449
46. Moretto, N., Facchinetti, F., Southworth, T., Civelli, M., Singh, D., and Patacchini, R. (2009) α,β-Unsaturated aldehydes contained in cigarette smoke elicit IL-8 release in pulmonary cells through mitogen-activated protein kinases. *Am. J. Physiol. Lung Cell. Mol. Physiol.* **296**, L839–L848
47. Daniele, R. P., Dauber, J. H., Altose, M. D., Dauber, J. H., Rowlands, D. T., Jr., and Gorenberg, D. J. (1977) Lymphocyte studies in asymptomatic cigarette smokers. *Am. Rev. Respir. Dis.* **116**, 997–1005
48. Lambert, C., McCue, J., Portas, M., Ouyang, Y., Li, J., Rosano, T. G., Lazis, A., and Freed, B. M. (2005) Acrolein in cigarette smoke inhibits T-cell responses. *J. Allergy Clin. Immunol.* **116**, 916–922
49. Cantin, A. M., North, S. L., Hubbard, R. C., and Crystal, R. G. (1987) Normal alveolar epithelial lining fluid contains high levels of glutathione. *J. Appl. Physiol.* **63**, 152–157
50. Van der Toorn, M., Smit-de Vries, M. P., Slebos, D.-J., de Bruin, H. G., Abello, N., van Oosterhout, A. J. M., Bischoff, R., and Kauffman, H. F. (2007) Cigarette smoke irreversibly modifies glutathione in airway epithelial cells. *Am. J. Physiol. Lung Cell. Mol. Physiol.* **293**, L1156–L1162
51. Dekhuijzen, P. N., Aben, K. K., Dekker, I., Aarts, L. P., Wielders, P. L., van Herwaarden, C. L., and Bast, A. (1996) Increased exhalation of hydrogen peroxide in patients with stable and unstable chronic obstructive pulmonary disease. *Am. J. Respir. Crit. Care Med.* **154**, 813–816
52. Huang, M. F., Lin, W. L., and Ma, Y. C. (2005) A study of reactive oxygen species in mainstream of cigarette. *Indoor Air* **15**, 135–140
53. Seys, L. J. M., Verhamme, F. M., Dupont, L. L., Desauter, E., Duerr, J., Seyhan Agircan, A., Conickx, G., Joos, G. F., Brusselle, G. G., Mall, M. A., and Bracke, K. R. (2015) Airway surface dehydration aggravates cigarette smoke-induced hallmarks of COPD in mice. *PLoS One* **10**, e0129897
54. Smaldone, G. C., Foster, W. M., O'Riordan, T. G., Messina, M. S., Perry, R. J., and Langenback, E. G. (1993) Regional impairment of mucociliary clearance in chronic obstructive pulmonary disease. *Chest* **103**, 1390–1396
55. Eklund, B.-M., Nilsson, S., Hedman, L., and Lindberg, I. (2012) Why do smokers diagnosed with COPD not quit smoking? A qualitative study. *Tob. Induc. Dis.* **10**, 17
56. Berlow, R. B., Dyson, H. J., and Wright, P. E. (2015) Functional advantages of dynamic protein disorder. *FEBS Lett.* **589** (19 Pt A), 2433–2440

Received for publication February 20, 2018.
Accepted for publication May 21, 2018.